Project acronym:	SACRA
Project title:	Spectrum and Energy Efficiency through multi-band Cognitive Radio
Project number:	European Commission – 249060
Call identifier:	FP7-ICT-2007-1.1
Start date of project:	01/01/2010 Duration: 36 months

Document reference number:	D2.3
Document title:	Design of space time frequency polarization codes
Version:	1.0
Due date of document:	Month M24 (December 2011)
Actual submission date:	12 January 2012
Lead beneficiary:	IT
Participants:	Abdelwaheb Marzouki (IT); Atso Hekkala (VTT)

Project co-funded by the European Commission within the 7th Framework Programme		
DISSEMINATION LEVEL		
PU	Public	X
PCA	Public with confidential annex	
CO	Confidential, only for members of the consortium (including Commission Services)	

EXECUTIVE SUMMARY

The main objective of the SACRA work package 2 (WP2) is to develop techniques and algorithms for cognitive energy efficient radio.

In particular, as specified in SACRA technical annex, the specific aim of Task 2.2 of WP2 is to focus on space time frequency coding schemes and to extend the code design criteria to include the polarization as a new component. In this deliverable the code design process has been carried out considering the existing space-time coding techniques which are used in 4G MIMO systems as LTE and beyond. Our efforts have been focused on the cognitive radio issue and especially on the set of physical layer procedures related to space-time coding helping cognitive radios to share the existing spectrum with primary users while introducing a minimum change on the existing systems and standards.

CONTENTS

1 INTRODUCTION

1.1 GENERAL CONTEXT

With the growing interest in cognitive radios several techniques have been proposed dealing with interference mitigation. Here we study the performance of orthogonal space time block codes (OSTBC) with the additional constraint consisting of reducing interference toward neighbouring users or primary users. We formulate the problem for minimizing the power received by the primary and secondary receivers while imposing a distorsionless condition on the received OSTC word and propose a solution based on these constraints.

Moreover, achieving spatial diversity in the low band TVWS is an issue in terms of antenna size and of antenna separation since an antenna separation distance of half a wavelength is necessary to avoid signal correlation and electromagnetic antenna coupling. This justifies the study of polarization based diversity as an alternative to spatial diversity for the SACRA use cases.

Our first task has been the investigation of the signalling techniques needed in such systems and under which the channel estimation and the advanced detection techniques can be carried out without difficulty. Our second concern is the development of precoding techniques allowing the existing space-time block coding scheme to be used without a substantial change on their structured properties. Thus powerful orthogonal design such the Alamouti scheme could be used in future cognitive radio systems despite their quasi-uniform spatial spectrum. Finally, our third concern is the use of polarization diversity jointly with space-coding. Our spatial filters are designed to take full advantage of the polarization as a new degree of freedom which may help to maintain an acceptable link level quality between secondary users while ensuring minimum interference to primary and secondary users.

Our Cognitive Radio (CR) specific transmission scheme is more realistic than some existing beamforming systems [Zhang08], in which prefiltering at secondary transmitter side supposes a perfect knowledge of the MIMO channel matrix between the secondary transmitter and the primary receiver terminals. In our work, only a MIMO correlation matrix is needed. Such a statistical feature does not need a special knowledge of the actual signal that is transmitted by primary user devices. Moreover, the existing scheme considers instantaneous signal vectors without any space-time code structure. This is very limiting since 4G systems make use essentially of codes that are structured either in time or in frequency and any arbitrary prefiltering that does not consider the special code structure may lead to the opposite effect and induce difficulties in reconstructing of the signal at the receiver side.

Our interference avoidance algorithm can be applied indifferently in space-time or space-frequency domains. In an OFDM based system such LTE, a space-time scheme can used in each narrow subcarrier before IFFT operation. Such an operation needs the use of different OFDM time symbols on a given subcarrier. The prefiltering can be applied on each vector of the space-time code word. The same prefiltering operation can be applied in space-frequency domain. In this case, space frequency block codes (SFBC) have to be used by replacing the time axis by the frequency axis. Such a coding is applied on neighbouring subcarriers instead of adjacent time symbols [Paul04]. More complex space-time-frequency coding such the Cyclic Delay Diversity (CDD) can be combined with our prefiltering scheme and applied without a difficulty. The ease of integration of the prefiltering scheme with different space-time-frequency coding combinations has allowed us to focus our analysis on the classical space-time space domain.

For channel estimation in MIMO communication, pilots are needed for all the channels between each transmit and receive antennas. This affects losses for data rate and spectral efficiency. In addition, large antenna arrays are unsuitable for mobile devices since uncorrelated MIMO channels require at least a half wavelength distance between each couple of co-polarized antennas. This is especially true when using lower carrier frequencies, as e.g. in TVWS bands. In order to prevent the data rate loss, concept of superimposed pilots has been proposed. In the superimposed pilot scheme, the pilots lay on the same carries as data and so data rates are not decreased. This is especially important when using large MIMO structures. However, some performance loss is expected. The use polarised antenna has been noticed to give a new promising dimension for MIMO communication. In the polarised MIMO, two conventional spatially separated single polarised antennas are replaced by one antenna structure having two orthogonal polarisations which helps avoiding cumbersome user equipments (UE) while benefiting of additional source of diversity and interference rejection capability. In addition, polarisation diversity is insensitive to frequency. Therefore, it could be especially suitable for MIMO communication in TVWS.

The rest of this deliverable is organized as follows. Section II presents the system description and channel model. Section III provides a channel estimation technique using superimposed pilots in the presence of Alamouti coding and polarised antennas. Some simulation results using the Winner II channel model are shown. Section IV details the MIMO prefiltering technique in presence of CR and exploiting polarization diversity at secondary link side. Finally, Section V concludes the deliverable.

1.2 PURPOSE OF THE DOCUMENT

This document is the deliverable D2.3 of WP2.3.1 entitled "Design of space time frequency polarization codes" of the FP7 SACRA project. It considers the studies on the space time coding techniques over the polarisation dimension. This deliverable is also related to WP2.3.2 where MIMO multiplexing techniques are considered as well as to WP4 where antennas including polarisation dimension are developed for SACRA terminal.

The goal of this document is to disseminate the studies regarding the space time polarisation coding techniques in a cognitive radio framework and to demonstrate their performances. This document intends also to give some useful inputs to WP2.3.2 and WP4 in terms of the use of polarised antennas in MIMO communications.

The signalling and interference avoidance algorithms developed in this report are mainly intended to meet a key objective of SACRA, which is the improvement of the spectral efficiency in a cognitive radio system.

2 SYSTEM DESCRIPTION

2.1 CHANNEL MODEL

For a MIMO system with N_t antennas at the transmitter side and N_r antennas at the receiver side, we can express the $N_r x N_t$ channel matrix in terms of the polarization channel response and the geometric configuration of the antennas at both sides of the link.

For 2D case, the most known to be complete MIMO channel model in terms of both scenarios and characterizations is the spatial channel model (SCM) that has been elaborated by 3GPP [3GPP TR 25.996] and which is derived mainly from the WinnerII channel model [WinnerII]. Despite its limitation to 2D case, this model is rich in terms of parameter calibration for simulation purposes.

Though 3GPP channel model is considered in our analysis, special attention has been focused on the distribution of each random parameter entering in the expression of this channel model. For instance e-NodeB related spatial parameter distributions are systematically modified in order to take into account the characteristics of our system, especially when dealing with indoor CR transmitter and receiver.

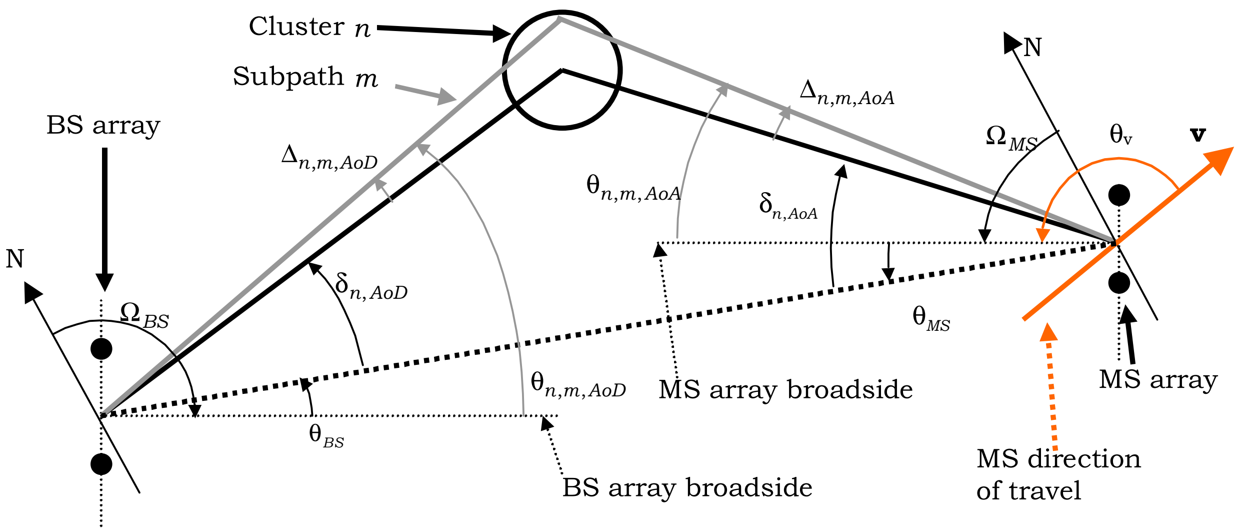

Figure 2.1. Path characteristics in the SCM model [3GPP TR 25.996].

The wideband channel impulse response between a pair of antennas u and s and along path n is a superposition of M sub-path channel responses given by

$$H_{u,s,n}(t,\tau)=\sqrt{\frac{P_n\sigma_{SF}}{M}}\sum_{m=1}^{m=M}\begin{pmatrix}\chi_{BS}^{v}(\theta_{n,m,AoD})\\ \chi_{BS}^{h}(\theta_{n,m,AoD})\end{pmatrix}^{T}\begin{bmatrix}e^{j\Phi_{n,m}^{v,v}} & \sqrt{r_{n,1}}e^{j\Phi_{n,m}^{v,h}}\\ \sqrt{r_{n,2}}e^{j\Phi_{n,m}^{h,h}} & e^{j\Phi_{n,m}^{h,v}}\end{bmatrix}\begin{pmatrix}\chi_{MS}^{v}(\theta_{n,m,AoA})\\ \chi_{MS}^{h}(\theta_{n,m,AoA})\end{pmatrix}\times$$
$$e^{jk\|v\|\cos(\theta_{n,m,AoA}-\theta_v)}e^{jkd_s\sin(\theta_{n,m,AoA})}e^{jkd_s\sin(\theta_{n,m,AoA})} \quad \textbf{Eq 1}$$

where:

$\chi_{\mathrm{BS}}^{(\mathrm{v})}(\theta_{\mathrm{n,m,AoD}})$ is the e-NodeB antenna complex response for the V-pol component.

$\chi_{\mathrm{BS}}^{(\mathrm{h})}(\theta_{\mathrm{n,m,AoD}})$ is the e-NodeB antenna complex response for the H-pol component.

$\chi_{\mathrm{MS}}^{(\mathrm{v})}(\theta_{\mathrm{n,m,AoA}})$ is the UE antenna complex response for the V-pol component.

$\chi_{\mathrm{MS}}^{(\mathrm{h})}(\theta_{\mathrm{n,m,AoA}})$ is the UE antenna complex response for the H-pol component.

$\left|\chi^{(.)}(.)\right|^2$ is the antenna gain

$\mathrm{r_{n1}}$ is the random variable representing the power ratio of waves of the nth path leaving the transmitter in the vertical direction and arriving at the receiver in the horizontal direction (v-h) to those leaving in the vertical direction and arriving in the vertical direction (v-v).

$\mathrm{r_{n2}}$ is the random variable representing the power ratio of waves of the nth path leaving the transmitter in the horizontal direction and arriving at the receiver in the vertical direction (h-v) to those leaving in the vertical direction and arriving in the vertical direction (v-v). The variables $\mathrm{r_{n1}}$ and $\mathrm{r_{n2}}$ are i.i.d.

$\Phi_{n,m}^{x,y}$ is the phase offset of the mth subpath of the nth path between the x component (either the horizontal h or vertical v) of the e-NodeB element and the y component (either the horizontal h or vertical v) of the UE element.

Winner II channel model [WinnerII] is used in section 3 in the channel estimation simulations in the presence of polarisation. This channel model has been developed in the EU research project called WINNER II. Its MATLAB model can be downloaded from the WINNER II project website. The channel model is planned to be used for simulations of radio systems beyond 3G, i.e. LTE and LTE-A. It covers frequency bands from 2 to 6 GHz having signal bandwidths up to 100 MHz. Based on several measurements campaigns, the channel model covers simulations of local, metropolitan, and wide area communication systems including both the link level and system level simulations. It has 11 different propagation indoor/outdoor (and LOS/NLOS) scenarios. The model covers SISO to multi-link MIMO scenarios. In addition, polarisation can also be included in the model. In general, modelling is done separately as a clustered delay line model.

Parameterisation is one of the advantageous features of the Winner II channel model. Through parameterisation, it is possible to use same modelling approach for e.g. indoor and outdoor environments as well as scenario dependent polarisation modelling.

In this work, B1 “Typical urban micro-dell” scenario is used in the simulations. Path loss option is turned off. In addition, NLOS scenario is used. Low mobility is assumed, i.e. the mobile speed is 3 m/s. Figure 2.2 shows the real part of the channel frequency response functions when the mobile speed is 3 m/s. It can be seen that the frequency response is almost constant over 32 OFDM symbols, i.e. the frame. That is the case even when the mobile speed is 20 m/s, see Figure 2.3.

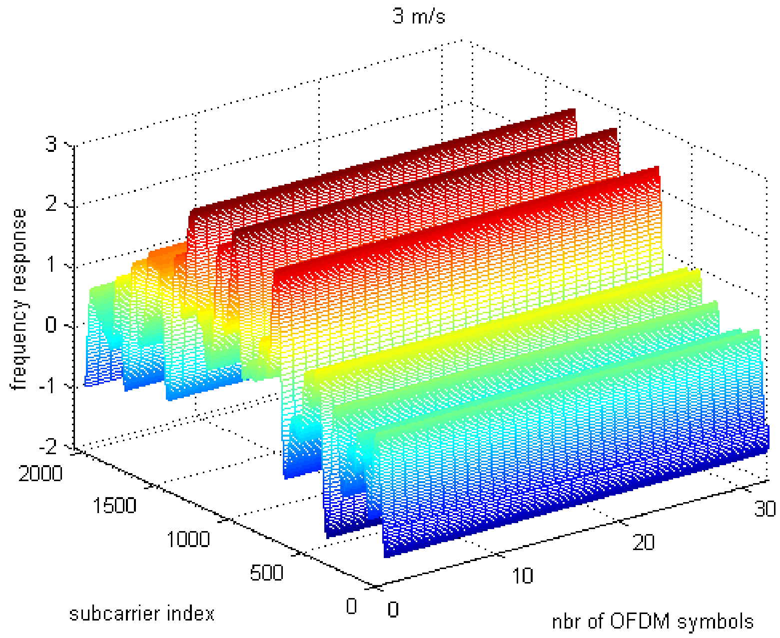

Figure 2.2. Channel frequency response functions for mobile speed 3 m/s.

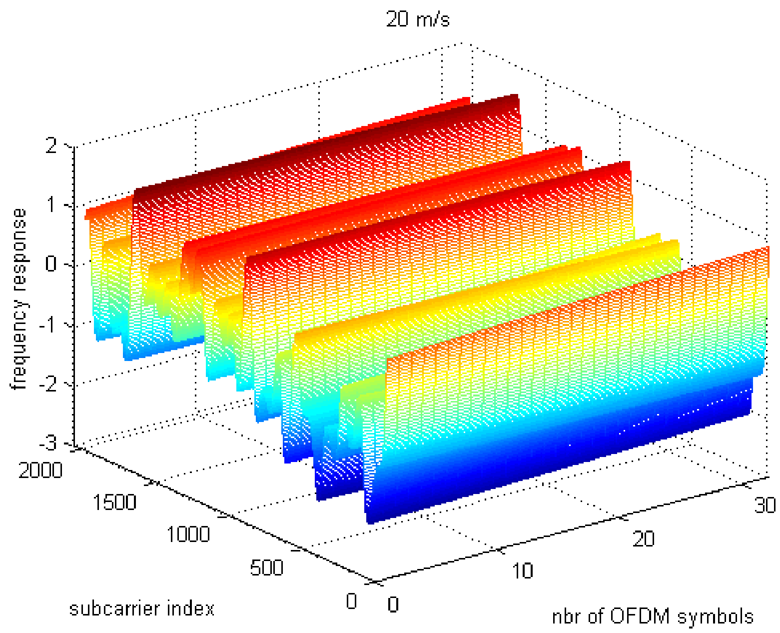

Figure 2.3. Channel frequency response functions for mobile speed 20 m/s.

Other parameters are generated in the Winner II channel model initialisation function as default. Vital OFDM system parameters used in the simulations can be found in Table 2.1.

Parameter	Value
Centre frequency	2 GHz
Bandwidth	100 MHz
Number of subcarriers	2048
Subcarrier spacing	48.828 kHz
Length of cyclic prefix	128
Symbol length	21.76 µs
Modulation	QPSK, 16QAM, 64QAM

Table 2.1. System parameters used in the simulations with Winner II channel model.

In this work, the polarisation option of the Winner II channel model is utilised. Half wavelength dipoles are used as antenna elements. Polarisation effects are achieved by slanting dipoles to ±45 degrees from vertical line. In addition, polarised arrays should be in use in the model. When using polarisation, the antennas can be located one upon the other. See Figure 2.4 clarifying simple two antenna configuration. In the figure, two antenna elements using single polarisation, i.e. conventional MIMO and dual polarisation, i.e. polarised MIMO are shown. In a similar way, four antenna elements could be used as two sets of two orthogonally polarised antenna elements.

Ideally, when the transmitter and receiver have dual polarised antennas in use, the cross-polar transmissions (e.g. from a vertically-polarized transmit antenna to a horizontally-polarized receive antenna) should be equal to zero [Oestges08]. However, this is not the case because of two depolarisation mechanisms. First, the antennas have imperfect cross-polar isolation (XPI). Second, the existence of a cross-polar ratio (XPR) in the propagation channel causes power leakage between orthogonal polarisations. When combining these effects, it yields to a global cross-polar discrimination (XPD).

In the simulations of this work, antennas are assumed to be ideal, i.e. their XPI is assumed very high. Mean value of the XPR and its variance in the B1 scenario (NLOS case) are set to 9 dB and 3 [WinnerII].

Figure 2.4. Two antenna elements for conventional MIMO (left) and polarised MIMO (right).

2.2 ORTHOGONAL SPACE TIME BLOCK CODE

Space time block codes (STBC) combine the transmit diversity across time and space by spreading the information in time and across the transmitting antennas while facilitating the information decoding at the receiver side. In orthogonal STBC (OSTBC) the vectors of the STBC matrices are designed in such a fashion that the vectors of the coding matrix are orthogonal in time and space yielding a simple linear decoding at the receiving terminal, so that no complex matrix manipulation such as inversion or singular value decomposition (SVD) is needed for recovering the information bit from the gathered received symbols. The disadvantage of OSTBC is a loss of spectral efficiency which in turn is partly compensated by a SNR gain and a simple receiver structure when compared to multiplexing techniques using fully the available degree of freedom of the channel. Moreover, the orthogonal design in space time coding makes it possible to combine the received symbols in an optimal way enhancing some QoS indicators such the probability of error and bit rate. Space time coding requires at least two transmitting antennas, whereas it is not necessary to have multiple arrays of receiving antennas, but the performance of the system may improve considerably with multiple receiving antennas [Tirkkonen02].

Assuming a narrow band flat block-fading channel model, we can write the relationship between the input and the output of a point-to-point MIMO system at any time t as

$$\mathbf{y}(\mathrm{t}) = \sqrt{\frac{\rho}{\mathrm{N_t}}}\mathbf{Hx}(\mathrm{t}) + \mathbf{n}(\mathrm{t}) \qquad \textbf{Eq 2}$$

where **H** is the $N_r x N_t$ complex channel matrix with unit variance and satisfying $E(tr(HH^H) = N_t Nr$, **y**(t) is a N_r size vector of the received signal, **x**(t) is a Nt size transmitted vector signal satisfying $E(\mathbf{x}^H\mathbf{x})=N_t$, and **n**(t) is a Nr size complex Gaussian noise vector with zero-mean and unit-variance. ρ is the SNR at each receive antenna.

Now, assuming that the channel is used at times t=1,...,T we can rewrite (Eq 2) as

$$\mathbf{Y} = \sqrt{\frac{\rho}{N_t}}\mathbf{HX} + \mathbf{N} \qquad \textbf{Eq 3}$$

where **Y** =[**y**(1),...,**y**(T)], **N** =[**n**(1),...,**n**(T)] and **X** =[**x**(1),...,**x**(T)].

Using an appropriate representation it has been shown [Tarokh99] that OSTBC can fall under the linear block coding. The linear representation of OSTBC is given as

$$\mathrm{X} = \sum_{\mathrm{k}=1}^{\mathrm{k}=\mathrm{K}} \Re\{\mathrm{s_k}\}\mathrm{C_k} + \Im\{\mathrm{s_k}\}\mathrm{D_k} \qquad \textbf{Eq 4}$$

where $\mathbf{C}_k$ and $\mathbf{D}_k$ are $N_t x K$ complex matrices, termed dispersion matrices and specifying the OSTBC, s_k k=1,...,K denote complex information symbols prior to space-time encoding.

Compared to arbitrary STBC, OSTBC has the following unitary property:

$$\mathbf{XX^H} = \left(\sum_{\mathbf{k}=1}^{\mathbf{k}=\mathbf{K}} |\mathbf{s_k}|^2\right)\mathbf{I} \qquad \textbf{Eq 5}$$

where $\mathbf{X}^H$ is the Hermitian matrix of $\mathbf{X}$.

As argued in [Shahbaz04] we introduce the “underline” operator for any matrix as

$$\underline{\mathbf{P}} = \begin{pmatrix} \mathrm{vec}(\Re\{\mathbf{P}\}) \\ \mathrm{vec}(\Im\{\mathbf{P}\}) \end{pmatrix} \qquad \textbf{Eq 6}$$

where vec is the vectorization operator stacking all columns of a matrix on top of each other. A compact vector

$$\underline{\mathbf{X}} = \mathbf{A}\underline{\mathbf{s}} \qquad \textbf{Eq 7}$$

The ($2N_tT$x$2K$) matrix **A** is defined as

$\mathbf{A} = \left[\underline{C_1},...,\underline{C_K}, \underline{D_1},...,\underline{D_K}\right]$

The advantage of the underlined vector notation is its compactness in one hand and its use in the precoding operation. Without precoding at the transmitter side, the input output vector form relationship is given by

$$\lambda^{qt,qr,qr'} = \mathrm{tr}\underline{Y^s} = \sqrt{\frac{\rho}{Nt}}\underline{\mathbf{H}_{eq}^s}\mathbf{A}\underline{\mathbf{s}} \qquad \textbf{Eq 8}$$

where

$$\mathbf{H}_{eq} = \begin{bmatrix} \Re\{\mathbf{I}_T \otimes \mathbf{H}\} & -\Im\{\mathbf{I}_T \otimes \mathbf{H}\} \\ \Im\{\mathbf{I}_T \otimes \mathbf{H}\} & \Re\{\mathbf{I}_T \otimes \mathbf{H}\} \end{bmatrix} \qquad \textbf{Eq 9}$$

in which $\mathbf{I}_T \otimes \mathbf{H}$ denotes the Kronecker product between the (TxT) identity matrix and the original complex MIMO channel matrix. Y is of size ($2N_rT$x1) while H_{eq} is a real matrix of size ($2N_rT$x$2N_tT$).

3 CHANNEL ESTIMATION USING SUPERIMPOSED PILOTS IN POLARISED MIMO SYSTEMS

In this section, we study channel estimation using superimposed pilots in the presence of Alamouti coding and polarised antennas. First, we introduce the superimposed pilots and the dual polarised antenna schemes. In addition, we present the Alamouti coding scheme and discuss its extension to the polarisation dimension. Then, we show some simulation results using the Winner II channel model introduced in the previous section.

3.1 SUPERIMPOSED PILOTS

The concept of the superimposed pilots was originally introduced already in 1965 for analog communications [Kastenholz65]. Later on the idea was applied the first time in digital communications in the year 1995 [Farhang-Boroujeny95]. Recently, it has received more interest, see e.g. [Huang09, Cui05, Chen06, Hiivala10].

In the concept of the superimposed pilots, the idea is, instead to have certain subcarriers dedicated for the pilots, to add the pilots on the data symbols. In other words, some of the subcarriers carry not only data but also pilot. Figure 3.1 clarifies more the superimposed pilot scheme and its difference to the conventional multiplexed pilot scheme. In the receiver side, the channel is estimated using the superimposed pilots and, if needed, interpolation between them is carried out. In practice, the estimation is done by averaging over several OFMD symbols to reduce interference caused by the actual data and to average out the noise. After that, estimated pilots can be subtracted away so that they are not disturbing the estimation of the actual data.

For the channel estimation, the LS estimates of the channel coefficients at subcarrier *k* can be given as [Hiivala10]

$$H_{LS}(k) = \frac{Y(k)}{P(k)}, \qquad k \in n + qT, \qquad q = 0,1, \dots C-1 \qquad \textbf{Eq 10}$$

where *Y* is the received signal, *P* is the known pilot sequence, and *T* is the distance between the pilots (16 subcarriers in this work). For averaging the estimated pilots over OFDM symbols, the channel is assumed to be (almost) constant over *M* OFDM symbols. The averaged channel estimates can then be given as

$$\boldsymbol{\hat{H}_{LS}(k) = \frac{1}{M}\sum_{m=1}^{M} H_{LS}\,(k,m)} \qquad \textbf{Eq 11}$$

In the case of this work, the averaging period of 32 OFDM symbols is used, see Figure 2.2 (and even Figure 2.3 where the mobile speed is 20 m/s). Finally, to get the channel estimates for the data carriers, simple and low complexity linear interpolation between the pilots in the frequency domain is carried out.

Compared to the conventional multiplexed pilot scheme, higher data rates and bandwidth efficiency are achieved when using the superimposed pilots. The difference even increases when number of transmit antennas increases. As an example, considering that in the conventional multiplexed pilot scheme with one transmit antenna and having 64 subcarriers for one symbol and four of them are pilot carriers, 93.75 % of the subcarriers can carry data. When there are four transmit antennas, only 75 % carriers carry data.

On the other hand, the use of the superimposed pilots causes performance degradation because some of the TX power must be allocated to the pilots and therefore poorer information SNR is achieved. In addition, the actual data interferes with channel estimation (because the data is underlying the pilots) and consequently removal of inaccurate pilots may affect performance losses. To decrease the performance degradation, iterative detection processes have been proposed, see e.g. [Cui05]. Here, it is assumed that the degradation is smaller with lower modulation orders. In [Huang09], it is mentioned that superimposed pilot schemes is suitable to broadcasting systems because in those systems no preamble is available for channel estimation. In addition, they mention that the superimposed schemes are suitable to timing and frequency synchronisation.

As mentioned above, some of the available transmit power should be allocated to the superimposed pilots. Power allocation factor β defines the ratio between the power allocated to the superimposed pilot sequence and the total transmitted power [Huang09]. Then the powers of data sequence ρ_s and superimposed pilot sequence ρ_p can be given by

$$\rho_s = (1-\beta)\rho \qquad \textbf{Eq 12}$$

$$\rho_p = \beta\rho \qquad \textbf{Eq 13}$$

where ρ is the total transmitted power. It is intuitively understandable that the channel estimation performance is dependent on power allocation factor β. There is a compromise between channel estimation accuracy and interference to data symbols / lower achievable SNR. For example, increasing β, better channel estimates are achieved but at the same time more interference to the data symbols is caused and lower achievable SNR for data estimation is received. In [Huang09], optimal β is studied. It can be noticed that the optimal β increases when the number of the OFDM symbols decreases and SNR increases. We assume that the optimal β is affected also by the used modulation method.

a)

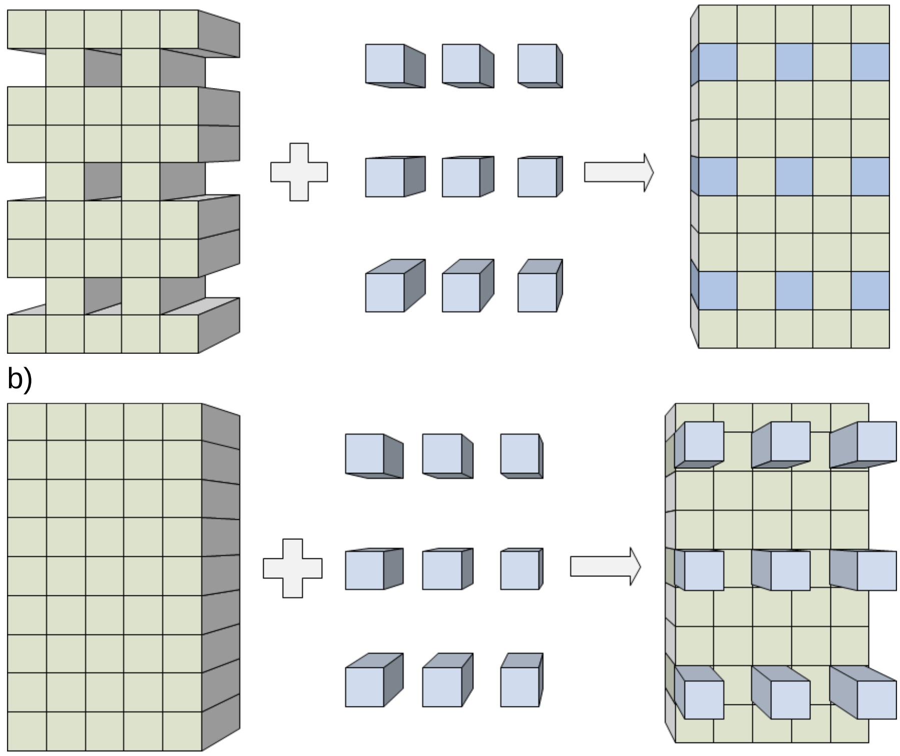

Figure 3.1. Principles of adding conventional (a) and superimposed (b) pilots.

3.2 ALAMOUTI CODING WITH POLARISED ANTENNAS

The first space time coding (STC) scheme for two transmit antennas was proposed in [Alamouti98]. This is nowadays called as Alamouti scheme. The aim of this scheme is to give full diversity in the spatial dimension without data rate loss. In addition to STC, space frequency coding could be used in the OFDM systems. However, in this work only STC is considered. When using the Alamouti scheme, channel state information does not need to be known in the transmitter. The transmission matrix for the Alamouti scheme can be given as

$$C_2 = \begin{bmatrix} s_1 & s_2 \\ -s_2^* & s_1^* \end{bmatrix} \qquad \textbf{Eq 14}$$

where s_1 and s_2 represent the first and second transmitted symbols. The rows and columns of the matrix represent the symbols transmitted from a particular antenna and the time each symbol is transmitted, respectively.

In [Tarokh99], the Alamouti scheme was generalised for more antennas. For example, for four antennas, the transmission matrix of the half rate code can be given as

$$\begin{bmatrix} s_1 & s_2 & s_3 & s_4 \\ -s_2 & s_1 & -s_4 & s_3 \\ -s_3 & s_4 & s_1 & -s_2 \\ -s_4 & -s_3 & s_2 & s_1 \\ s_1^* & s_2^* & s_3^* & s_4^* \\ -s_2^* & s_1^* & -s_4^* & s_3^* \\ -s_3^* & s_4^* & s_1^* & -s_2^* \\ -s_4^* & -s_3^* & s_2^* & s_1^* \end{bmatrix} \qquad \textbf{Eq 15}$$

where symbols, rows, and columns are defined the same as in (Eq 14). See also Section 2.2 where OSTBC is discussed.

In conventional MIMO communication, antenna elements should be placed away from each other to achieve low enough correlations between the channels. In [Nabar02, Ahn04], it is stated that the distance between antennas should be at least one signal wavelength. This may affect difficulties to utilise larger MIMO structures especially in handhelds. Particularly, this is an issue when operating in low frequencies e.g. in TVWS. Also the cost issue may become a problem [Nabar02].

The use of polarised antennas has been seen a promising alternative for cost- and space-effective MIMO communication, see e.g. [Nabar02], [Ahn04], [Kilic09], [Deng05]. Instead using two separate antennas in the transmitter and receiver, in the dual polarised systems, two data streams have been transmitted using two orthogonal polarisations of one antenna. Figure 2.4 clarifies the difference between the conventional MIMO antenna and the dual polarised antenna configuration.

In [Nabar02], the Alamouti scheme is studied and utilised in polarisation dimension. Each of the symbol stream is transmitted using different orthogonal polarisations. Then, in the receiver side, the streams are Alamouti decoded. In [Kilic09], the work is extended to have virtual 4x4 MIMO. That means they have two antennas and both of them are with dual polarisations. Another approach to employ the polarisation is presented in [Deng05]. They have also two transmit antennas with dual polarisations, but they utilise the Alamouti coding for the data stream from the different antennas having the same polarisation. That is they can use the Alamouti scheme for two information sequences. In the receiver, they are able to separate the two sequences received by different polarisations.

In this work, we follow the scheme presented in [Nabar02]. We have virtual 2x2 MIMO. That means we utilise two polarised antennas both in the transmitter and receiver sides. And Alamouti coding over polarisation is used. See Figure 3.2 for more clarification of the scheme.

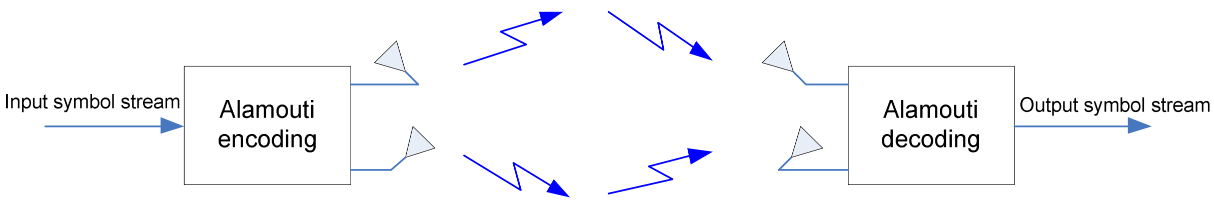

Figure 3.2. Block diagram of the Alamouti scheme used in this work.

3.3 RESULTS

3.3.1 PAPR

High peak-to-average power ratio (PAPR) of the transmitted signal is one of the most severe problems in the use of the OFDM. It leads to power inefficient transmissions. When using the superimposed pilots, the PAPR may increase even more. It is intuitively understandable that PAPR of the signal may increase when adding more power to some of the OFDM subcarriers. In [Chen06], this problem is considered. They mention that selecting the superimposed pilots judiciously, the PAPR increases only a little, it can even decrease with higher power allocation factor (β). That is because the properly selected pilots increase the average power and do not affect so much to peak power of the OFDM signal. However, as stated earlier, it should be noted that the use of the higher power allocation factors leaves lower power available for the actual data carriers (if the total transmitted power is fixed to a certain value). This may cause performance degradations. The PAPR problem in general and PAPR reduction techniques are studied in WP4/5 of the SACRA project.

It is stated in the literature (see e.g. [Huang09]) that the best performance of the channel estimation is obtained when the superimposed pilots are equally spaced in the frequency domain and they have equal power. On the other hand, by intuition, the equally spaced pilots (even if they have random values) may increase the PAPR of the OFDM signal generating high peaks to time domain signal due to symmetry properties of FFT. Therefore, it would be interesting to study that is it possible to achieve PAPR reduction using not equally spaced pilots and on the other hand how much performance degradation is noticed.

We study how the PAPR of the OFDM signal is affected by using different sets of the superimposed pilots (β=0.25). First, we use equal power and equally spaced (in frequency domain) pilots, i.e. the pilots are located on every 16th carrier. Using randomly selected pilots the PAPR of the signal is not (at least noticeable) increased, instead it could be even decreased. Figure 3.3 shows an example on the PAPR of the one OFDM symbol. As can be seen, using the QPSK modulated pilots with the same values, regular high peaks are generated to the signal. On the other hand, the pilots with random values decrease the PAPR of the original signal.

Then we use equal power and in frequency domain randomly spaced pilots. Actually, the pilot spaces are randomly set between 13 and 18 subcarriers. The number of the pilots is the same as in the previous case. Now, when comparing to the previous case, it can be seen that in the worst case scenario (i.e. the pilots with the same values), the PAPR is reduced. However, using the random value pilots, the PAPRs are actually the same. Figure 3.4 shows an example of PAPRs using randomly spaced pilots. In this specific example, the randomly spaced pilots actually give higher PAPR. As a conclusion of this study, we can say that properly selecting the set of the superimposed pilots, the increase of the PAPR is not a real problem in the transmitted signal. In addition, there is no need to set the pilots randomly in frequency domain. Instead, it is reasonable to use equally spaced pilots to achieve the best possible performance, as stated in [Huang09].

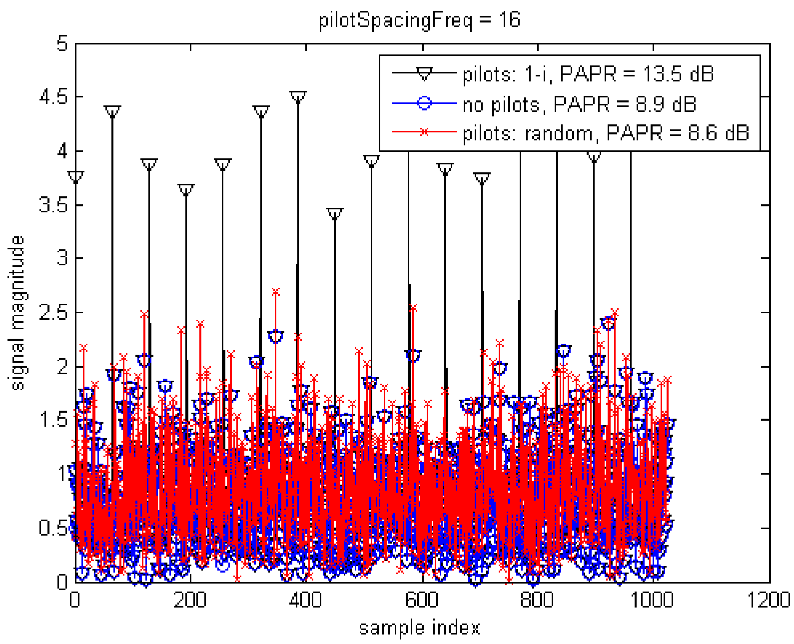

Figure 3.3. PAPR of the signal using equally spaced superimposed pilots.

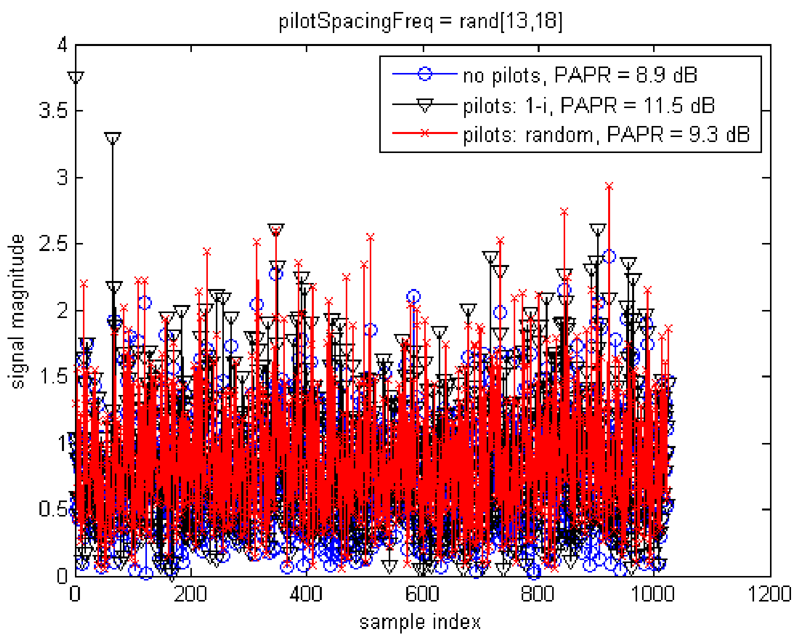

Figure 3.4. PAPR of the signal using randomly spaced superimposed pilots.

3.3.2 Channel estimation

Considering the superimposed pilots, it is important to study optimal power allocation factor β. In [Huang09], it is stated that optimal β depends on the used channel estimation method (the optimal β is larger for LS than MMSE), received SNR (higher the SNR higher the optimal β), and numbers of averaged OFDM symbols *M* (higher the *M* lower the optimal β). In [Chen06], it is mentioned that optimal β for QPSK modulation is 0.3.

We study the optimal β in the presence of the dual polarised antennas, i.e. the polarised MIMO. In addition, comparisons to the conventional MIMO, i.e. single polarised antennas, cases are done. Figure 3.6 shows simulated BERs as a function of β using different modulation methods in the presence of single and dual polarised antennas. We notice that optimal β depends on the used modulation method. For QPSK the optimal β is ~0.15, for 16QAM it is ~0.25, and for 64QAM even higher, i.e. ~0.3. Considering the polarisations and the optimal β, no differences can be seen between the conventional and polarised MIMO cases. However, in general, with dual polarised antennas, better BERs are achieved.

Figure 3.5 shows BERs as a function of β using QPSK modulation with different SNRs. As can be seen, higher the SNR larger the optimal β is. In addition, with high SNR the difference between the conventional and polarised MIMO cases is more visible.

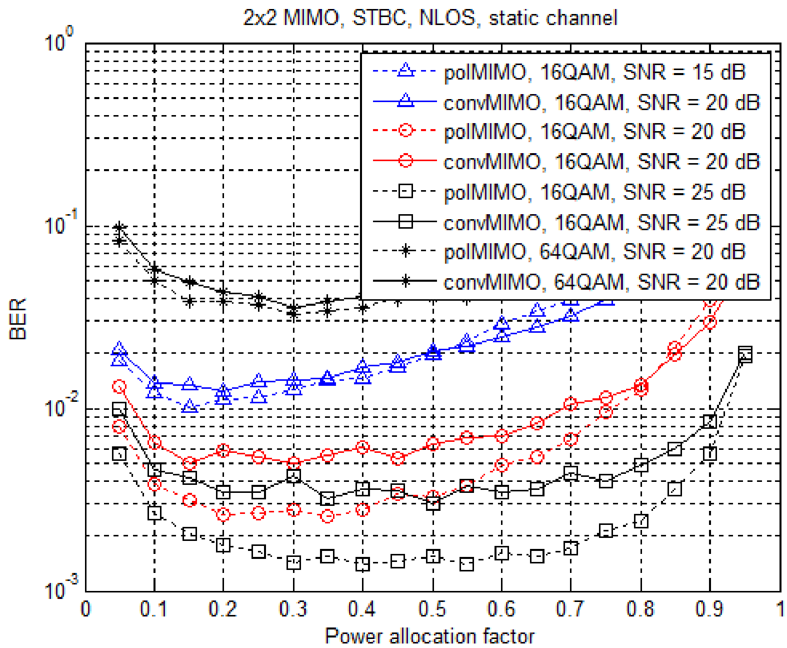

Figure 3.5. BER vs. power allocation factor using 16QAM and 64QAM modulations.

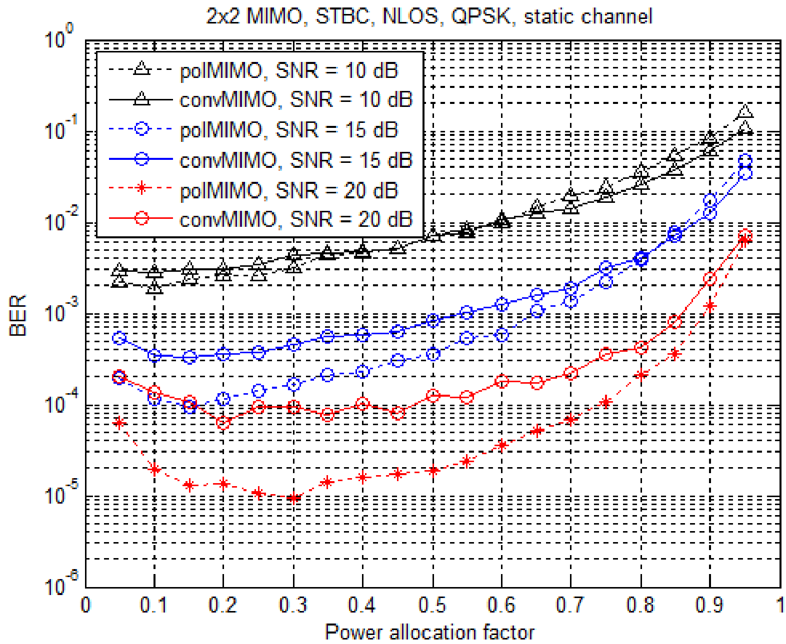

Figure 3.6. BER vs. power allocation factor using QPSK modulation with different SNRs.

Then we study the performance of the channel estimation based on the superimposed pilots. In particular, we compare the performances in the presence of the single and dual polarised antennas. Figure 3.7 shows the BER curves using different modulation methods. As can be seen, the error floor is increased when the modulation order is increased. It is well known that the performance degradations may occur due to the fact that the pilots and data lie on the same carriers and interfere with each other. This degradation even increases when the modulation order is increased. It seems that it is not reasonable to use the superimposed pilots with high modulation orders. On the other hand, using the polarised MIMO, the error floor is always lower than using the conventional MIMO.

It is important to study more the performance degradation due to the superimposed pilots and compare it to the conventional multiplexed pilot system. The tested multiplexed pilot system has pilots on every 16th subcarriers (just same as in the superimposed scheme) placed on every 4th OFDM symbol. Similar LS channel estimation is processed for both of the schemes. Figure 3.8 shows the superimposed and conventional multiplexed pilots comparison using QPSK modulation. As can be seen, the performances are almost the same.

Finally, we perform some comparisons between the superimposed and multiplexed pilot schemes, see Figure 3.9 and Figure 3.10. It can be clearly seen that the use of the superimposed pilots affect performance degradation. However, considering the most interesting parts of the curves, i.e. around BER of 10^{-2}, the performance differences are about 3-4 dB. In addition, it seems that almost the same performance is achieved in the presence of both the static and time variant channels. That is because we have low mobility scenario with the mobile speed of 3 m/s and therefore the channel stays anyway almost constant over the frame, see Figure 2.2.

Moreover, when comparing these results to the results using perfect channel state information (PCSI) at the receiver, it can be noticed that the use of the LS channel estimation degrades the performance about 3-4 dB at BER of 10^{-2}

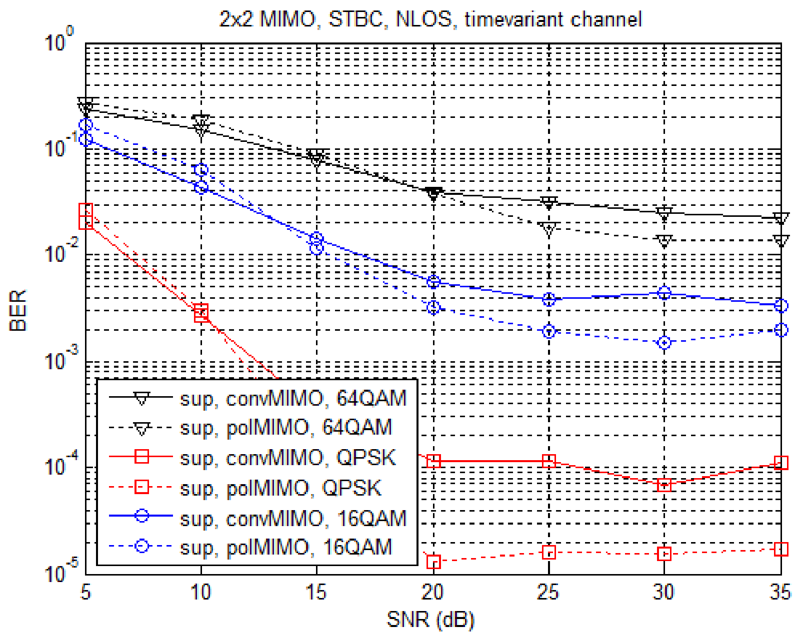

Figure 3.7. BER using different modulation methods.

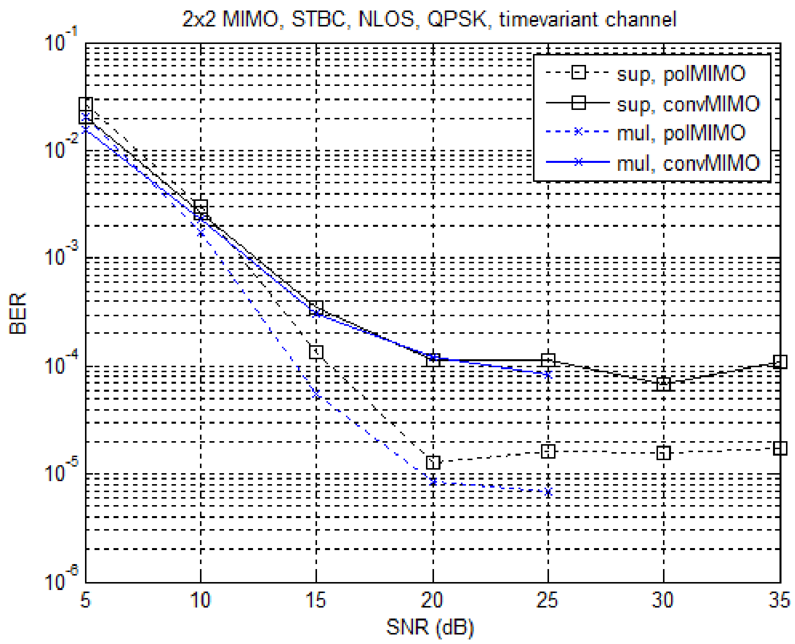

Figure 3.8. BER comparisons between superimposed and multiplexed pilots using QPSK.

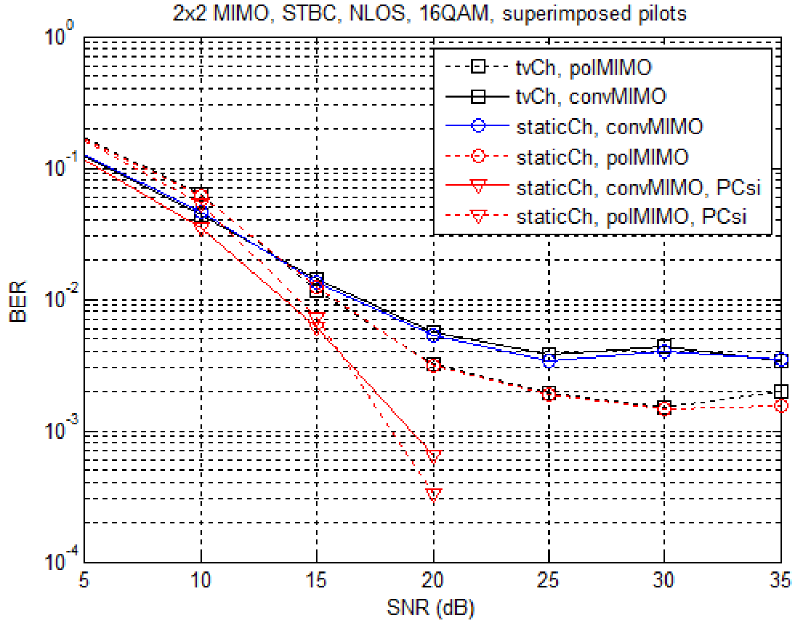

Figure 3.9. BER curves for superimposed pilots using 16QAM.

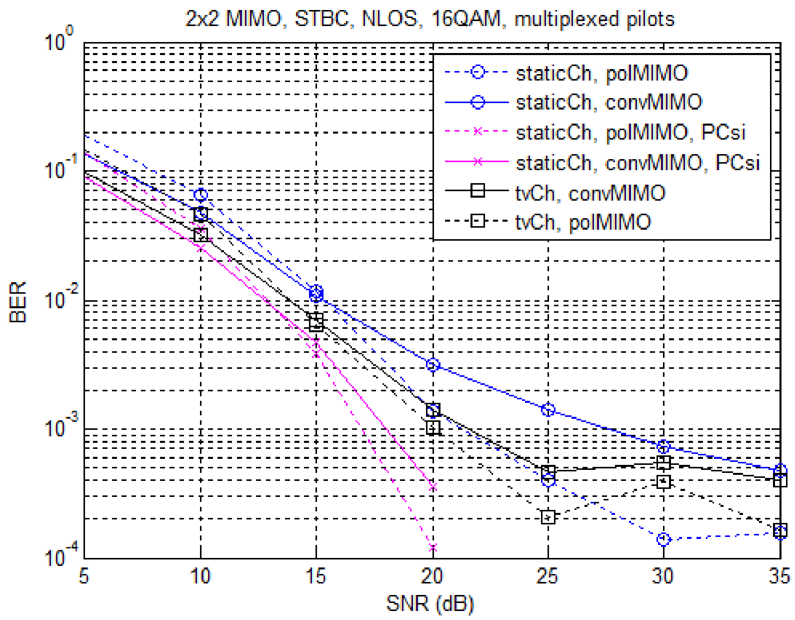

Figure 3.10. BER curves for multiplexed pilots using 16QAM.

3.4 CONCLUSION

In this section, the channel estimation using the superimposed pilots in the polarised MIMO system was studied. As the cost- and space-efficient option, the polarised antennas were considered. The Alamouti coding was utilised over polarisation dimension. Higher data rate and bandwidth efficiency were achieved using the superimposed pilots than the conventional multiplexed pilots. The difference is even larger when the number of the antennas is high. Due to the use of the superimposed pilots, some performance degradations were noticed. For example, it was not seen reasonable to use the superimposed pilots with 64QAM. However, the difference between the superimposed and multiplexed pilot schemes was insignificant with the small modulation orders. In addition, the optimal power allocation factor β was seen to be dependent on the used modulation order. Finally, it was noticed that it is reasonable to utilise the superimposed pilots in a low mobility scenario because the channel stays almost constant during the frame (and so the channel estimates can be averaged over the frame).

4 SPACE TIME CODING WITH INTERFERENCE AVOIDANCE

4.1 INTRODUCTION

With the growing interest in cognitive radios several techniques have been proposed dealing with interference mitigation. Here we study the performance of orthogonal space time block codes (OSTBC) with an additional constraint of reducing interference to neighbouring users or primary users. The secondary transmitter (ST) is transmitting to a secondary receiver (SR) in the presence of a number of primary users (PU). The ST is transmitting in the frequency of primary users. We formulate the problem for minimizing the power received by the primary while keeping the power received by the secondary receiver equal to a certain threshold and propose a solution based on those constraints.

We combine polarization selection and prefiltering matrix estimation at the CR terminals side and we show that a substantial Signal to Noise ratio (SNR) gain can be obtained compared to a system using a singular polarization mode.

4.2 SYSTEM MODEL

We consider a CR system based on a secondary transmitter (ST) with N_t antennas and a secondary receiver (SR) with N_r receive antennas. Each antenna is supposed to be equipped with a polarization switching capability so it can operate indifferently on vertical or horizontal polarization mode. Although little meaning at this stage of analysis we adopt the channel model in Section 2 in which D signal waves are impinging on the receiver from D different directions and originating from one or more users. These directions are available at the ST as a set of steering vectors $\mathbf{a}_i$ where i=1..,D. This allows us to adopt MIMO system model between the secondary transmitter and the set of primary nodes in which each angle of arrival is associated to a virtual user, so the MIMO channel between the secondary transmitter and the set of virtual primary nodes may be modelled by a Ntx x d matrix **H**p.

Without a loss of generality, we suppose that the primary network system is a TDD mode like, so spatial primary spectrum can be sensed by the secondary transmitter.

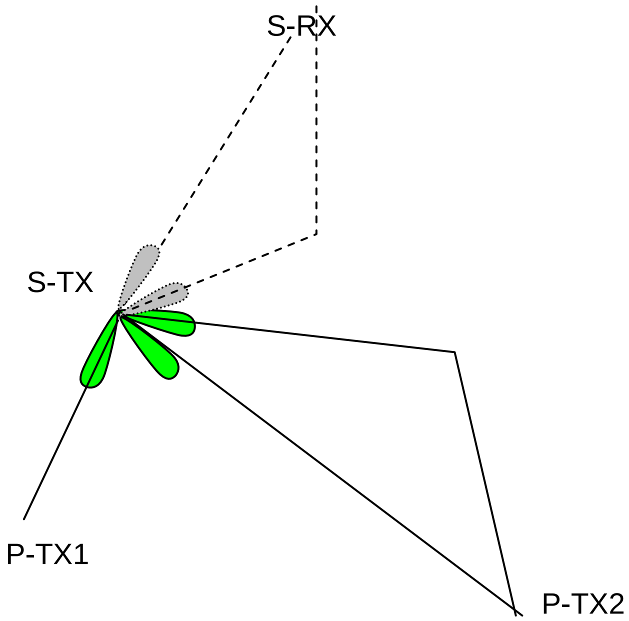

Figure 4.1. Interference avoidance in cognitive radio systems.

4.3 PRECODING OPERATION

When precoding is used at the transmitter side, the system model already presented in Section 2 needs to be modified by the precoding operation and also duplicated to represent the Secondary-Secondary (SS) link and secondary-primary (SP) link. Moreover for each of such links some constraints have to be satisfied in order to respect the interference power on the primary link, the maximum allowed transmitted power and QoS parameters.

In our space-time block coding the data sequence is broken into K substreams that are the chosen from, constellation and passed through a STC mapper performing the following operation:

- Polarization mode selection
- OSTC selection
- Precoding operation

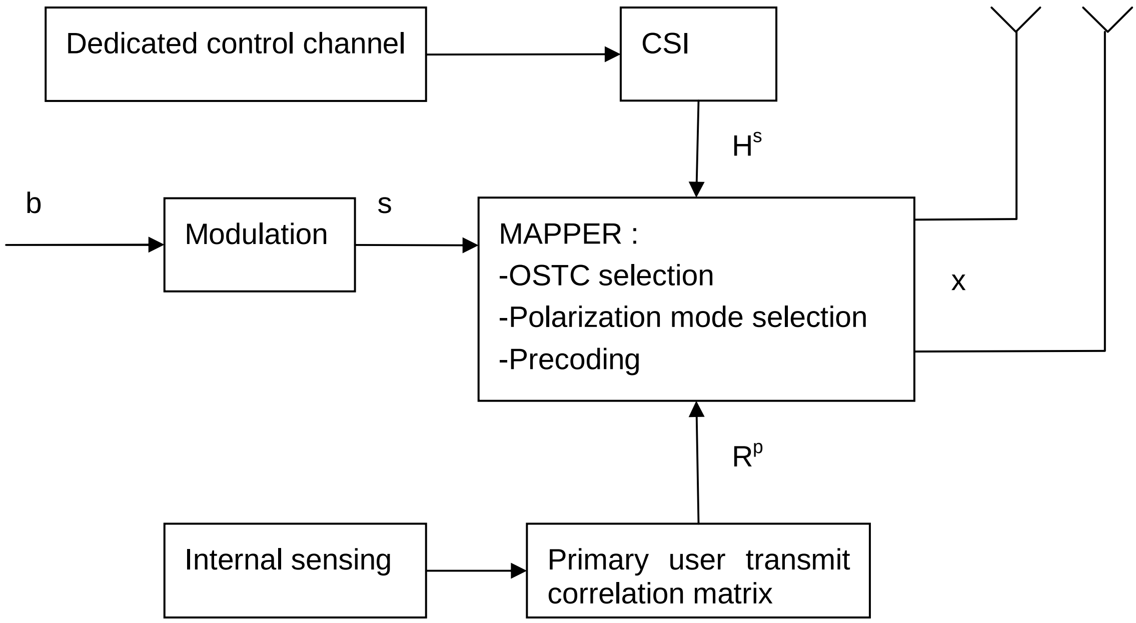

Figure 4.2. Block diagram of space time block coding.

4.3.1 SS system model

The most advanced TX-RX design relies on the introduction of weighting matrix at the receiver side. Minimum Variance Linear Receivers have been already proposed for multiuser interference mitigation [Hassibi02, Shahbaz04] and are based on the underlined vector signal presentation. When such a processing is conducted at the transmitter side, the precoding techniques are usually designed for unstructured codes, i.e codes without a special space-time structure. Filtering techniques such the well know SVD based filtering, MMSE filters and other multiuser MIMO interference cancellation techniques are characterised by some flexibility since relying on covariance matrices of signal vectors and not on their structure as it should be the case for OSTBC.

Our concern is the precoded signal model with a precoding matrix acting on the entry of the OSTBC compact dispersion matrix **A**. Let qt (resp. qr) be the polarization mode at the transmitter side (resp. at the receiver side), we may write the underlined input-output relationship as:

$$\underline{\mathbf{Y}^{s,qt,qr}} = \sqrt{\frac{\rho_s}{Nt}}\underline{\mathbf{H}_{eq}^{s,qt,qr}}\mathbf{W}\mathbf{A}\underline{\mathbf{s}} + \underline{\mathbf{N}} \qquad \textbf{Eq 16}$$

When operating at the receiver side, a straightforward approach for estimating the transmitted signal is to use the following soft output vector:

$$\underline{\hat{\mathbf{s}}} = \mathbf{A}^T \mathbf{H}_{eq}^{s,qt,qr^{\mathbf{T}}} \underline{\mathbf{Y}^{s,qt,qr}} = \sqrt{\frac{\rho_s}{Nt}} \mathbf{A}^T \mathbf{H}_{eq}^{s,qt,qr^{\mathbf{T}}} \underline{\mathbf{H}_{eq}^{s,qt,qr}} \mathbf{W}\mathbf{A}\underline{\mathbf{s}} + \mathbf{A}^T \mathbf{H}_{eq}^{s,qt,qr^{\mathbf{T}}} \underline{\mathbf{N}} \qquad \textbf{Eq 17}$$

Clearly a powerful approach conserving OSTBC structure in one hand and performing channel matching on the other hand is to set up the following equality constraint during the optimisation procedure:

$$\mathbf{A}^T \mathbf{H}_{eq}^{s,qt,qr^{\mathbf{T}}} \underline{\mathbf{H}_{eq}^{s,qt,qr}} \mathbf{W}\mathbf{A} = \alpha \mathbf{I}_{2\mathrm{K}} \qquad \textbf{Eq 18}$$

where α is a constant that can be adjusted to satisfy additional power constraints.

On the other hand a maximum transmitted power constraint has to be respected by any communication system. It is standard system dependent and can be formulated as

$$\frac{\rho_s}{Nt} tr(\mathbf{W}^{\mathbf{T}}\mathbf{W}) \leq \rho_{s,max} \qquad \textbf{Eq 19}$$

Eq 18 and Eq 19 provide the SS communication link constraints that are needed in the precoding design. To completely specify this design, one has to take into account the SP link.

4.3.2 SP system model

The SP link system model can be formulated using the same approach used in SS link. In particular if qt and qr' are respectively the polarization mode at the transmitter side and at the receiver side, we may write the underlined input-output relationship as:

$$\underline{\mathbf{Y}^{p,qt,qr\prime}} = \sqrt{\frac{\rho_p}{Nt}} \underline{\mathbf{H}_{eq}^{p,qt,qr}} \mathbf{W}\mathbf{A}\underline{\mathbf{s}} + \underline{\mathbf{N}} \qquad \textbf{Eq 20}$$

where $\mathbf{H}_{eq}^{p,qt,qr\prime}$ is the MIMO channel matrix between the secondary transmitter and the primary receiver. ρ_p is the undesired SNR that may affect in some extent the performance of the primary receiver if no precoding is realised.

The objective is therefore to find out the precoding matrix and also the polarization modes to be used at both ends of the SS link so the following objectives are reached at the same time: an interfering power minimized at the primary receiver side and a SNR maximised at the secondary receiver side. We restrict our analysis to a random SP MIMO channel in which the only estimated parameter is the transmit correlation matrix, given by

$$\mathbf{R}_{eq}^{p,qt,qr\prime} = E\left(\mathbf{H}_{eq}^{p,qt,qr\prime^T} \mathbf{H}_{eq}^{p,qt,qr\prime}\right) \qquad \textbf{Eq 21}$$

Such a matrix can be estimated easily during the sensing step, by correlating the received signal vector with itself at secondary user side. We henceforth assume the SP transmit correlation matrix know at the transmitter side.

Given a transmit polarization mode q_t, the interference power to be minimized can be written

$$\mathrm{p}^{p,qt} = \frac{\rho_s}{Nt} tr\left(\mathbf{W}^T \mathbf{R}_{eq}^{p,qt,qr\prime}\mathbf{W}\right) \qquad \textbf{Eq 22}$$

4.3.3 Minimum variance algorithm

The polarization mode at the primary receiver side is supposed not to be controllable by the secondary system. Only the precoding matrix and the polarization modes on the secondary link are subject to optimization. Gathering together the above minimisation criteria and constraints we can set the optimization problem as follows

$$\left(\widehat{W}, \widehat{qt}, \widehat{qr}\right) = arg \min_{qr,qt,\prime W} \frac{\rho_s}{Nt} tr\left(\mathbf{W}^T \mathbf{R}_{eq}^{p,qt,qr\prime}\mathbf{W}\right) \qquad \textbf{Eq 23}$$

$$s.t: tr\ \left(\mathbf{A}^T \mathbf{H}_{eq}^{s,qt,qr^{\mathbf{T}}} \underline{\mathbf{H}_{eq}^{s,qt,qr}} \mathbf{W}\mathbf{A} - \alpha \mathbf{I}_{2\mathrm{K}}\right) = 0 \qquad \textbf{Eq 24}$$

We proceed as follows

- Find the four precoding matrices $\widehat{\mathbf{W}}^{qt,qr}$ qt=v,h;qr=qt satisfying Eq 22 and Eq 23
- For each of the estimated precoded matrices, choose the polarization mode and the transmit power satisfying the following three criteria and constraints:
    - Maximum SNR at the secondary receiver side
    - Respecting the transmit power system related power constraint
    - Satisfying the maximum allowed threshold at the primary receiver side

To find the four precoding matrices, we make use of the Lagrange multiplier method. The Lagrangian function for this problem can be written as

$$L(W, \Lambda) = \frac{\rho_s}{Nt} tr\left(\mathbf{W}^T \mathbf{R}_{eq}^{p,qt,qr\prime}\mathbf{W}\right) - tr\left(\mathbf{\Lambda}^{\mathrm{T}}\left(\mathbf{A}^T \mathbf{R}_{eq}^{s,qt,qr} \mathbf{W}\mathbf{A} - \alpha \mathbf{I}_{2\mathrm{K}}\right)\right) \qquad \textbf{Eq 25}$$

where

$$\mathbf{R}_{eq}^{s,qt,qr} \triangleq \mathbf{H}_{eq}^{s,qt,qr^{\mathbf{T}}} \mathbf{H}_{eq}^{s,qt,qr} \qquad \textbf{Eq 26}$$

and $\mathbf{\Lambda}$ is a (2Kx2K) matrix of Lagrange multipliers. Differentiating this function with respect to **W**, equating it to zero and making use of the distortionless constraint yields the following precoder,

$$\widehat{\mathbf{W}}^{qt,qr} = \alpha \mathbf{R}_{eq}^{p,qt,qr'^{-1}} \mathbf{R}_{eq}^{s,qt,qr} \mathbf{A} \mathbf{Q}^{\mathrm{qt,qr,qr'}} \mathbf{A}^T \qquad \textbf{Eq 27}$$

where:

$$\mathbf{Q}^{\mathrm{qt,qr,qr'}} = \left(\mathbf{A}^T \mathbf{R}_{eq}^{s,qt,qr} \mathbf{R}_{eq}^{p,qt,qr'^{-1}} \mathbf{A} \right)^{-\mathbf{1}} \qquad \textbf{Eq 28}$$

The total interference power on the primary receiver is given by

$$\widehat{\mathrm{p}}^{qt,qr,qr'} = \frac{\rho \alpha^2}{Nt} \lambda^{\mathrm{qt,qr,qr'}} \qquad \textbf{Eq 29}$$

Where

$$\lambda^{\mathrm{qt,qr,qr'}} = \mathrm{tr}(\mathbf{Q}^{\mathrm{qt,qr,qr'}}) \qquad \textbf{Eq 30}$$

The SNR at the secondary receiver side is given by

$$\widehat{\mathrm{SNR}}^{qt,qr,qr'} = \frac{\rho \alpha^2 \gamma^{\mathrm{qt,qr,qr'}}}{Nt} \qquad \textbf{Eq 31}$$

where:

$$\gamma^{\mathrm{qt,qr,qr'}} = \mathrm{tr}\left(\mathbf{Q}^{\mathrm{qt,qr,qr'}} \mathbf{A}^T \left(\mathbf{R}_{eq}^{s,qt,qr} \mathbf{R}_{eq}^{p,qt,qr'^{-1}} \right)^2 \mathbf{R}_{eq}^{s,qt,qr} \mathbf{A} \mathbf{Q}^{\mathrm{qt,qr,qr'}} \right) \qquad \textbf{Eq 32}$$

Finally the actual transmitted power is given by

$$\widehat{\mathrm{P}}_{\mathrm{t}}^{qt,qr,qr'} = \frac{\rho \alpha^2 \delta^{\mathrm{qt,qr,qr'}}}{Nt} \qquad \textbf{Eq 33}$$

where

$$\delta^{\mathrm{qt,qr,qr'}} = \mathrm{tr}\left(\mathbf{Q}^{\mathrm{qt,qr,qr'}} \mathbf{A}^T \mathbf{R}_{eq}^{s,qt,qr} \mathbf{R}_{eq}^{p,qt,qr'^{-2}} \mathbf{R}_{eq}^{s,qt,qr} \mathbf{A} \mathbf{Q}^{\mathrm{qt,qr,qr'}} \right) \qquad \textbf{Eq 34}$$

Let η be the allowable interference threshold. From the inequality constraints: $\hat{\mathrm{p}}^{qt,qr,qr'} \leq \eta$ and $\widehat{\mathrm{P}}_{\mathrm{t}}^{qt,qr,qr'} \leq \rho$, it is easily verified that the scaling parameter α is to be set equal to:

$$\alpha = \boldsymbol{min}\left(\sqrt{\frac{N_t}{\delta^{\mathrm{qt,qr}}}}, \sqrt{\frac{N_t\eta}{\rho\lambda^{\mathrm{qt,qr}}}}\right) \qquad \textbf{Eq 35}$$

The final resulting SNR is therefore given by:

$$\widehat{\mathrm{SNR}}^{qt,qr,qr'} = \boldsymbol{min}\left(\frac{\rho}{\delta^{\mathrm{qt,qr,qr'}}}, \frac{\eta}{\lambda^{\mathrm{qt,qr,qr'}}}\right)\gamma^{\mathrm{qt,qr,qr'}} \qquad \textbf{Eq 36}$$

Finally, the optimisation over transmit and receive polarization mode over the SS link is achieved by maximizing Eq 36 as follows:

$$(\widehat{qt,qr}) = \arg\max_{qt,qr} \boldsymbol{min}\left(\frac{\rho}{\delta^{\mathrm{qt,qr,qr'}}}, \frac{\eta}{\lambda^{\mathrm{qt,qr,qr'}}}\right)\gamma^{\mathrm{qt,qr,qr'}} \qquad \textbf{Eq 37}$$

In general the primary receiver polarization is unknown. In this case the correlation matrix becomes random and only an average of the SNR over the correlation matrix may be obtained. Since the rotation of the primary receiver is unknown such a primary receiver polarization is no longer discrete, so the SNR average has to be taken over the rotation matrix RV via the SP correlation matrix. In 2D, the rotation matrix is uniquely identified by the polarization tilt angle β, so one may write the average SNR as:

$$\widehat{\mathrm{SNR}}^{qt,qr} = \mathrm{E}_{\mathrm{qr'}}\left(\widehat{\mathrm{SNR}}^{qt,qr,qr'}\right) = \int \widehat{\mathrm{SNR}}^{qt,qr,qr'(\beta)}\mathrm{p}(\beta)d\beta \qquad \textbf{Eq 38}$$

where p(β) is the distribution of the tilt angle. In this expression, the tilt angle is supposed equal to zero when the antennas are oriented along the z axis, which corresponds to the vertical polarization mode case.

4.3.4 Effect of imperfect CSI

Imperfect CSI is the most limiting issue in MIMO wireless communication. In particular a polarized MIMO system may take various limitation forms. We distinguish here two limitation factors which can be handled easily by our approach: lack of sufficient pilot signal on the SS link, making it impossible to estimate the channel response in the reverse link and unknown polarization mode at the secondary receiver side.

The first limitation is handled thanks to the special constraint (Eq 24) which is expressed not as function of the MIMO channel matrix on itself as it is the case in almost all existing systems but as a function of a product between the channel matrix and its Hermitian conjugate, which makes its generalization to unknown channel simple and obvious. So a new constraint can be written when only an average of the transmit MIMO correlation matrix is known in the form

$$\mathbf{A}^T \mathrm{E_H}\left(\mathbf{R}_{eq}^{s,qt,qr}\right)\mathbf{R}_{eq}^{s,qt,qr}\mathbf{W}\mathbf{A} = \alpha\mathbf{I}_{2\mathrm{K}} \quad \textbf{Eq 39}$$

The quantity $\mathrm{E_H}\left(\mathbf{R}_{eq}^{s,qt,qr}\right)$ can be evaluated at the received side during several symbols and transmitted back on a low bandwidth pilot channel. The transmit correlation matrix is principally function of the set of path powers and the angle of departure (AOD). These quantities are known to be slowly varying in time since due to specular reflection by objects with size of several wavelengths.

4.4 NUMERICAL RESULTS

This section presents some simulation results reproducing the common existing systems. We simulate the performances of both C2 and C4 OBTC (Eq 12 and Eq 13) and we consider various channel scenarios and equipment capabilities.

4.4.1 Polarization diversity analysis

We present here some simulation results illustrating the performances of our interference avoidance for different polarization modes under different multipath scenarios. We assess the impact of the SNR threshold constraint on the measured SNR at the secondary receiver side by examining the behaviour of such a SNR by varying the maximum allowed power while fixing the threshold level. In absence of a primary system, such a relationship is obviously linear in transmitted power. However, the presence of the threshold factor introduces a non-linearity dependence effect that is expressed by Eq 36. During our simulation work, the system parameters are set as follows:

- The SNR threshold perceived by a primary system receiver is chosen equal to 0 dB.
- The MIMO channel matrices are normalized for both SP and SS links. The effect of different SS and SP shadowing effects can be well considered by a simple scaling of the ratio between the transmitted power and the threshold.
- The number of secondary transmitter antennas is equal to 2.
- The number of primary receiver antennas is equal to 2.
- The number of secondary receiver antennas is equal to 1.
- The number of spatial paths on the SP link is fixed to 4. No further subpaths around the four main paths are considered in our simulation. Finally, the polarized MIMO channel matrix is provided by the 3GPP SCM channel model.
- The XPD value is equal to 8 dB

Figures 4.3 depict the behaviour of the resulting SNR at secondary receiver side for different polarization modes and assuming a single path on the SS link. Figure 4.4 depicts the same results under four paths. In order to examine the results more clearly, logarithmic scale has been used on the two axes.

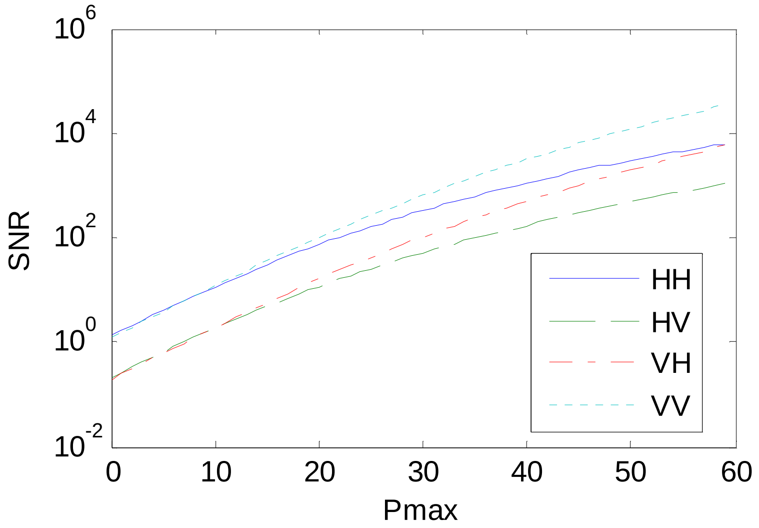

Figure 4.3. SS SNR versus maximum system power for different polarization modes and under one path scenario

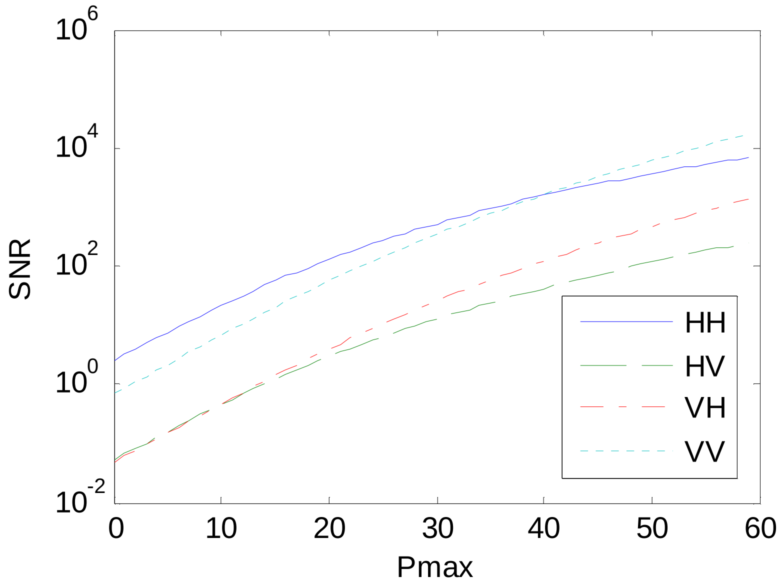

Figure 4.4. SS SNR versus maximum system power for different polarization modes and under four paths scenario

For both channel scenarios, a linear increase of the resulting SNR is obtained when the difference between the maximum power and the threshold is below 20 dB. A gain of 8 dB is obtained when the same polarization is used at both ends of SS link. This value is obviously equal to the XPD value. The latter is usually dependent on the propagation conditions.

4.4.2 SNR versus number of antennas

In our second simulation we assess the performances of the proposed schema for different values of the number of transmitting antennas. Figure 4.5 shows the average of reached SNR with respect to maximum transmitter power for two cases. In the first case the number of transmitting antenna is equal to 2 and a C2 OSTBC is used. In the second case, the number of transmitting antenna is equal to 4. For this case, we have used a C4 OSTBC. In the two cases, the number of receiving antennas on the SS link is chosen equal to one, while the number of receiving antennas on the SP link is chosen equal to 4 in order to favour a channel rank equal to 4 on the SP link and give the minimum variance method its full sense. The number of paths on the SP link is chosen equal to 6 as suggested by the 3GPP model favouring in the same time a full rank condition. On the SS link, the number of paths is chosen equal to 2. VV polarization mode is chosen in both cases.

The SNR saturation which is observed in the previous results when the number of transmitting antennas is equal to 2 is naturally found in this simulation. The novelty is the quasi linearity behaviour with 4 transmitting antennas, showing that a CR system could coexist without a difficulty with a primary system in such a case.

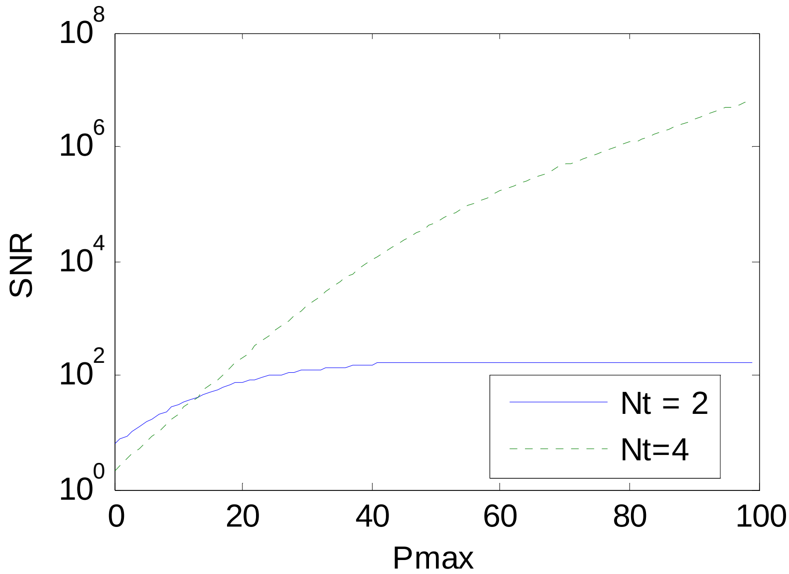

Figure 4.5. SS SNR versus maximum system power for different transmitter antennas assuming VV polarization mode, four six paths scenario

4.5 CONCLUSION

In this section the problem of precoder design using convex optimization for a secondary user using space time block codes was addressed. The novelty of our works lies in the fact that interference constraint and SNR optimization of the secondary system is achieved while preserving space time code structure.

Results have shown high interference avoidance capability when both polarization selection and four transmitting antennas are used. Threshold setting on SP link has been shown to be the main limiting factor when only two antennas are used by the secondary transmitter, despite the appreciable gain that is brought by polarization selection.

5 CONCLUSIONS

In this report space time polarization coding techniques in a cognitive radio framework have been proposed and their performances have been tested.

As far as feasibility and integration in future systems are concerned, we have proposed signalling and channel estimation using superimposed pilots in a polarised MIMO system in which Alamouti coding was utilized over polarization dimension. Results have shown that using the superimposed pilots higher data rate and bandwidth efficiency can be achieved than conventional multiplexed pilots.

One of the main contributions in this deliverable is to provide prefiltering technique allowing the use of conventional OSTBC in a cognitive radio scenario. The prefiltering technique has been optimized for the purpose of minimizing the interference that a secondary system may introduce on an existing primary system. Results have shown powerful interference avoidance capability of the proposed prefiltering technique. Polarization diversity has been used to allow achieving better SNR on the secondary link while keeping the induced interference below threshold.

6 ACRONYMS

Term	**Description**
2D	2 Dimensions
3D	3 Dimensions
3GPP	3rd Generation Partnership Project
BER	Bit Error Rate
BS	Base station
CR	Cognitive Radio
CRx	Cognitive Receiver
CDD	Cyclic Delay Diversity
CTx	Cognitive Transmitter
DOA	Direction of Arrival
FDD	Frequency Division Multiplexing
FFT	Fast Fourier Transform
LOS	Line of Sight
LS	Least Squares
LTE	Long Term Evolution
LTE-A	Long Term Evolution – Advanced
MIMO	Multiple Inputs Multiple Outputs
MMSE	Minimum Mean Square Error
MS	Mobile Station
MT	Mobile Terminal
NLOS	Non Line of Sight
OFDM	Orthogonal Frequency Division Multiplexing
OSTBC	Orthogonal Space Time Block Coding
PAPR	Peak-to-Average Power Ratio
PCSI	perfect channel state information
PRx	Primary Receiver
PTx	Primary Transmitter
PU	Primary User
QAM	Quadrature Amplitude Modulation

Term	**Description**
QoS	Quality-of-Service
QPSK	Quadrature Phase-Shift Keying
Rx	Receiver
SCM	Spatial Channel Model
SFBC	Space Frequency Block Coding
SISO	Single Input Single Output
SNR	Signal to Noise Ratio
SP	Secondary-Primary link
SR	Secondary Receiver
SS	Secondary-Secondary link
ST	Secondary Transmitter
STBC	Space Time Block Coding
SVD	Singular Value Decomposition
SU	Secondary User
TDD	Time Division Multiplexing
TVWS	TV White Spaces
Tx	Transmitter
WP	Work Package
XPD	Cross-Polar Discrimination
XPI	Cross-Polar Isolation
XPR	Cross-Polar Ratio

7 REFERENCES

[3GPP TR 25.996] 3GPP TR 25.996, “Spatial channel model for Multiple Input Multiple Output (MIMO) simulations” (Release 9).

[Alamouti98] S. M. Alamouti, “A simple transmit diversity technique for wireless communications,” IEEE Journal on Selected Areas on Communications, vol. 15, no. 8, October 1998, pp. 1451-1458.

[Ahn04] C.-J. Ahn, Y. Kamio, S. Takahashi, and H. Harada, "Reverse link performance improvement for an wideband OFDM using Alamouti coded heterogeneous polarization antennas," Computers and Communications, ISCC 2004 Proceedings, vol. 2, Jun. 2004, pp. 702-707.

[Chen06] N. Chen, G. T. Zhou, “Superimposed training for OFDM: a peak-to-average power ratio analysis,” IEEE Transactions on Signal Processing, vol. 54, no. 6, June 2006, pp. 2277-2287.

[Cui05] T. Cui and C. Tellambure, “Superimposed pilot symbols for channel estimation in OFDM systems,” in Proceedings GLOBECOM, vol. 4, pp. 2229-2233, December 2005.

[Deng05] Y. Deng, A. Burr, and G. White, “Performance of MIMO systems with combined polarization multiplexing and transmit diversity," in Proceedings IEEE VTC, vol. 2, no. 30 May 2005, pp. 869-873.

[Farhang-Boroujeny95] B. Farhang-Boroujeny, “Pilot-based channel identification: Proposal for semi-blind identification of communication channels,” Electronics Letters, vol. 31, no. 13, June 1995, pp. 1044-1046.

[Hassibi02] B. Hassibi and B. M. Hochwald, “High-rate codes that are linear in space and time,” IEEE Trans. Inform. Theory, vol. 48, pp. 1804–1824, July 2002.

[Hiivala10] M. Hiivala, I. Harjula and M. Lasanen, “Low complexity channel estimation for superimposed pilots in distributed OFDMA systems”, in Proceedings WTS, pp. 1-6 April 2010.

[Huang09] W.-C. Huang, C.-P. Li and S.-J. Li, ”On the power allocation and system capacity of OFDM systems using superimposed training schemes,” IEEE Transactions on Vehicular Technology, vol. 58, no. 4, May 2009, pp. 1731-1740.

[Kastenholz65] C. E. Kastenholz and W. P. Birkemeier, ”A simultaneous information transfer and channel-sounding modulation technique for wide-band channels,” IEEE Transactions on Communication Technology, vol. 13, no. 2, June 1965, pp. 162-165.

[Kilic09] Y. Kilic, M. Loca, and E. Anarim, “Space-time polarization diversity in multiple-input multiple output communication systems,” in Proceedings AFRICON 2009.

[Nabar02] R. U. Nabar, H. Bo□lsckei, V. Erceg, D. Gesbert, and A. J. Paulraj, "Performance of multiantenna signaling techniques in the presence of polarization diversity," IEEE Transaction on Signal Processing, vol. 50, no. 10, Oct. 2002, pp. 2553-2562.

[Oestges08] C. Oestges, B. Clerckx, M. Guillaud, and M. Debbah, “Dual-polarized wireless communications: From propagation models to system performance evaluation,” IEEE Transaction on Wireless Communications, vol. 7, no. 10, Oct. 2008, pp. 4019–4031.

[Paul04] A. Paulraj, D. Gore, R. Nabar, and H. Bolcskei. “An overview ofMIMO communications a key to gigabit wireless,” Proceedings of the IEEE, vol. 92, pp. 198–218, Feb. 2004.

[Shahbaz04] S. Shahbaz Panahi, M. Beheshti, A. B. Gershman, M. Gharavi-Alkhansari, and K. M. Wong, “Minimum variance linear receivers for multi-access MIMO wireless systems with space-time block coding,” IEEE Transactions on Signal Processing, vol. 52, pp. 3306-3313, Dec. 2004.

[Tarokh99] V. Tarokh, H. Javarkhani and Calderbank, “Space-time block codes from orthogonal designs,” IEEE Transactions on Information Theory, vol. 45, no. 5, July 1999, pp. 1456-1467.

[Tirkkonen02] O. Tirkkonen and A. Hottinen, \Square-matrix embeddable space-time block codes for complex single constellations," IEEE Trans. Inf. Theory, vol. 48, no. 2, pp. 384-395, Feb. 2002.

[WinnerII] P. Kyösti, et al., "WINNER II channel models," IST-WINNER D1.1.2, Sep. 2007. Available: https://www.ist-winner.org/WINNER2-Deliverables/D1.1.2v1.1.pdf.

[Zhang08] R. Zhang and Y.-C. Liang, "Exploiting multi-antennas for opportunistic spectrum sharing in cognitive radio networks", IEEE J. Sel. Topics Sig. Proces., vol. 2, no. 1, pp. 88–102, Feb. 2008.